Inorganic Chemistry
Communication

Inorg. Chem. 2010, 49, 6799–6801 6799
DOI: 10.1021/ic1009175

Theoretical Calculation of the Magnetic Resonance Parameters of Trigonal-Prismatic Tris(*o*-aminobenzenethiol)technetium and -rhenium Complexes

Simon C. Drew,*,† John Baldas,‡ and John F. Boas‡,§

†*Max Planck Institut für Bioanorganische Chemie, 45470 Mülheim an der Ruhr, Germany,*
‡*Australian Radiation Protection and Nuclear Safety Agency, Lower Plenty Road, Yallambie, Victoria 3085, Australia, and* §*School of Physics, Monash University, Victoria 3800, Australia*

Received May 7, 2010

Spin Hamiltonian parameters for the neutral trigonal-prismatic $Tc(abt)_3$ and $Re(abt)_3$ chelates (abt = *o*-aminobenzenethiol) are calculated using relativistic density functional theory at the all-electron level. The small magnitude of the calculated *g* shifts and metal hyperfine interactions is in excellent agreement with previous experimental predictions based upon a ligand-centered ground-state magnetic orbital. The theoretical ^{14}N ligand hyperfine and quadrupole couplings also reproduce the nuclear frequencies measured by electron spin-echo envelope modulation spectroscopy. The nuclear quadrupole interaction of ^{187}Re is predicted to be 2 orders of magnitude larger than that of ^{99}Tc, in agreement with empirical simulation of the continuous-wave electron paramagnetic resonance spectrum. The spectrum of $Tc(abt)_3$ at high solute concentrations contains a central resonance not predicted for the isolated complex by theoretical calculations. The absence of this resonance at low solute concentrations provides evidence of intermolecular interactions in these systems.

Alkyl-substituted dithiolenes are strong π-electron donors and can stabilize metals in high oxidation states. Recent concentration has been on complexes of nickel, molybdenum, and tungsten in view of their relationship to important enzymes and possible applications in materials science.[1] A recent advance in the theoretical study of heavy-metal complexes has been the ability to properly treat relativistic effects at the all-electron level and at one consistent level of density functional theory (DFT).[2] By inclusion of higher-order spin−orbit coupling (SOC) effects, the empirical spin Hamiltonian (SH) parameters obtained from experimental electron paramagnetic resonance (EPR) spectroscopy of molybdenum dithiolene systems can be accurately predicted from DFT.[3] However, to our knowledge, there are no theoretical studies of the magnetic resonance parameters of complexes of the $4d^1$ and $5d^1$ metals technetium and rhenium with dithiolenes and related ligands. The trigonal-prismatic complexes of technetium and rhenium with the ligands *o*-phenylenediamine (*o*-pda), *o*-aminobenzenethiol (abt), benzenedithiol (bdt), toluene-3,4-dithiol (tdt), and *cis*-1,2-diphenylethene-1,2-dithiol (pdt) form a series in which coordination to the metal varies from 6N to 3N3S to 6S and in which the organic ring system in the second coordination sphere varies in complexity. Their EPR spectra are characterized by *g* anisotropies and metal hyperfine interactions[4−10] much smaller than those found for tetragonal technetium and rhenium complexes[11] and have been interpreted as arising from delocalization of the unpaired electron over the entire ligand π system.[5,6,8] Here we report relativistic DFT calculations of the SH parameters for the metal and coordinating ^{14}N ligands that predict the key features of the EPR spectra of $Tc(abt)_3$ and $Re(abt)_3$. We then compare these predictions with the SH parameters obtained through empirical simulation of the experimental continuous-wave (CW)- and pulsed-EPR spectra.

The starting coordinates for the calculations were taken directly from the published crystallographic structures of $Tc(abt)_3$[12] and $Re(abt)_3$,[9] with the molecular *Z* axis defined to lie along the approximate C_3 symmetry axis (Figures 1a and 2a). Using the *ORCA* program,[13] the spin-unrestricted

*To whom correspondence should be addressed. E-mail: drew@mpi-muelheim.mpg.de. Tel: +49-208-306-3865. Fax: +49-208-306-3951.

(1) Karlin, K. D., Stiefel, E. I., Eds. *Progress in Inorganic Chemistry, Vol. 52, Dithiolene Chemistry: Synthesis, Properties, and Applications*; Wiley: New York, 2004.
(2) Cosper, M. M.; Neese, F.; Astashkin, A. V.; Carducci, M. D.; Raitsimring, A. M.; Enemark, J. H. *Inorg. Chem.* **2005**, *44*, 1290–1301.
(3) (a) Drew, S. C.; Young, C. G.; Hanson, G. R. *Inorg. Chem.* **2007**, *46*, 2388–2397. (b) Drew, S. C.; Hill, J. P.; Lane, I.; Hanson, G. R.; Gable, R. W.; Young, C. G. *Inorg. Chem.* **2007**, *46*, 2373–2387. (c) Drew, S. C.; Hanson, G. R. *Inorg. Chem.* **2009**, *48*, 2224–2232.
(4) Stiefel, E. I.; Gray, H. B. *J. Am. Chem. Soc.* **1965**, *87*, 4012–4013.
(5) Stiefel, E. I.; Eisenberg, R.; Rosenberg, R. C.; Gray, H. B. *J. Am. Chem. Soc.* **1966**, *88*, 2956–2966.
(6) Al-Mowali, A. H.; Porte, J. *J. Chem. Soc., Dalton Trans.* **1975**, 250–252.
(7) (a) Kawashima, M.; Koyama, M.; Fujinaga, T. J. *Inorg. Nucl. Chem.* **1976**, *38*, 801–805. (b) Kirmse, R.; Stach, J.; Spies, H. *Inorg. Chim. Acta* **1980**, *45*, L251–L253.
(8) Baldas, J.; Boas, J. F.; Bonnyman, J.; Pilbrow, J. R.; Williams, G. A. *J. Am. Chem. Soc.* **1985**, *107*, 1886–1891.
(9) Danopoulos, A. A.; Wong, A. C. C.; Wilkinson, G.; Hursthouse, M.; Hussain, B. *J. Chem. Soc., Dalton Trans.* **1990**, 315–331.
(10) Borisova, L. V.; Prasolova, O. D.; Evtikova, G. A.; Marov, I. N. *Zh. Neorg. Khim.* **1990**, *35*, 944–950.
(11) (a) Lack, G. M.; Gibson, J. F. *J. Mol. Struct.* **1978**, *46*, 299–306. (b) Baldas, J.; Boas, J. F.; Williams, G. A. *Appl. Magn. Reson.* **1996**, *11*, 499–508.
(12) Baldas, J.; Boas, J.; Bonnyman, J.; Mackay, M. F.; Williams, G. A. *Aust. J. Chem.* **1982**, *35*, 2413–2422.
(13) Neese, F. *ORCA: An ab initio, DFT and Semiempirical Electronic Structure Package*, version 2.4, revision 26; Max-Planck Institut für Bioanorganische Chemie: Mülheim, Germany, 2005.

Published on Web 06/25/2010

Table 1. SH Parameters of $Re(abt)_3$ and $Tc(abt)_3$ Calculated from Theory and Their Comparison with Empirical Simulation of Experimental Data[a]

	method	g_{xx}	g_{yy}	g_{zz}	$\langle g\rangle^b$	A_{xx}	A_{yy}	A_{zz}	$\langle A\rangle^c$	Q_{xx}	Q_{yy}	Q_{zz}
$Tc(abt)_3$	expt [d]	2.0080	2.0080	2.0073	2.0078	−8.7	−8.7	12.2	−1.7			< 0.6
	BP86	2.0100	2.0085	2.0075	2.0086	−8.8	−9.2	1.2	−5.6	−0.17	−0.24	0.41
	B3LYP	2.0129	2.0110	2.0098	2.0112	−7.9	−8.8	21.7	1.6	−0.19	−0.27	0.46
$Re(abt)_3$	expt [d,e]	2.0080	2.0080	2.0020	2.0060	−34.0	−34.0	4.0	−21.3	26.0	26.0	−52.0
	BP86	2.0069	2.0059	2.0022	2.0050	−25.3	−26.8	−6.8	−19.6	20.9	25.6	−46.5
	B3LYP	2.0133	2.0112	2.0068	2.0104	−30.9	−33.2	8.6	−18.5	23.8	28.7	−52.5

[a] Hyperfine and quadrupole couplings are given for ^{99}Tc and ^{187}Re in units of 10^{-4} cm^{-1}. Euler angles and additional A and Q parameters of ligand ^{14}N nuclei appear in Table S1 (Supporting Information). [b] $\langle g\rangle = (g_{xx} + g_{yy} + g_{zz})/3$. [c] $\langle A\rangle = (A_{xx} + A_{yy} + A_{zz})/3$. [d] Uncertainties in principal g, A, and Q values for ^{187}Re are ±0.002, $\pm 2 \times 10^{-4}$ cm^{-1}, and $\pm 1 \times 10^{-4}$ cm^{-1}, respectively. Uncertainties in principal g and A values for ^{99}Tc are ±0.0015 and $\pm 0.5 \times 10^{-4}$ cm^{-1}, respectively. [e] Corresponds to natural abundance: $g_n(^{187}Re)/g_n(^{185}Re) = 1.010$; $Q(^{187}Re)/Q(^{185}Re) = 0.950$.

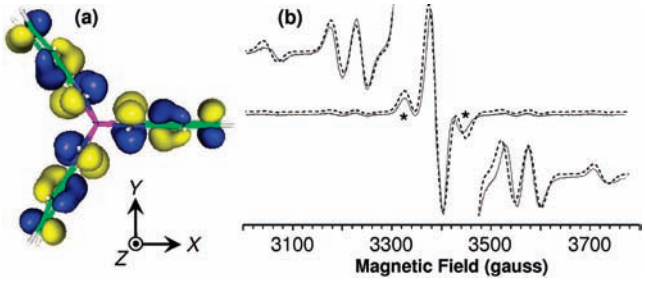

Figure 1. (a) Structure of the $Re(abt)_3$ complex and contour plot of the singly occupied molecular orbital calculated at the B3LYP level of theory (surfaces drawn at ±0.025 au). (b) Experimental (—) and simulated (– –) X-band CW-EPR spectra of 1 mM $Re(abt)_3$ in DMF at 130 K, 9.524 GHz, and 2 mW. Shoulder features are indicated by asterisks. Empirical simulation parameters are compared with theory in Table 1.

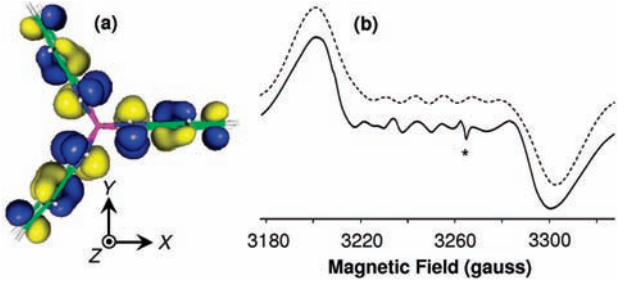

Figure 2. (a) Structure of the $Tc(abt)_3$ complex and contour plot of the singly occupied molecular orbital calculated at the B3LYP level (surfaces drawn at ±0.025 au). (b) Experimental (—) and simulated (– –) X-band CW-EPR spectra of 0.5 mM $Tc(abt)_3$ in 9:1 DMF/$CHCl_3$ at 120 K and 9.139 GHz (the experimental spectrum was reproduced from ref 8). An asterisk denotes an experimental artifact. Empirical simulation parameters are compared with theory in Table 1.

Kohn−Sham equations were solved self-consistently for a $S = {}^1/_2$ ground state of the neutral complexes, using either a pure (BP86) or hybrid (B3LYP) functional. A large, fully decontracted well-tempered basis set[14] and high numerical integration accuracy were employed to ensure flexibility in the core region for accurate predictions of the nuclear hyperfine (**A**) and quadrupole (**Q**) couplings. Scalar relativistic effects were treated at the all-electron level using the zeroth-order regular approximation.[15] The **g** and (^{187}Re/ ^{99}Tc) **A** matrices were computed using a coupled-perturbed self-consistent-field formalism and a SOC operator derived from an accurate mean-field method. Full details are given in the Supporting Information.

The theoretical computations confirm early experimental evidence that the unpaired electron resides in a $2a_2'$ ligand-centered molecular orbital (Figures 1a and 2a and S3 in the Supporting Information).[5,6,8,16] Commensurate with this, the g shifts from the free electron value are also small and the best theoretical values generally deviate in magnitude from experiment by < 0.002 (Table 1). The ^{99}Tc and ^{187}Re nuclear hyperfine couplings are likewise very small because of the low spin density at the metal ion (Table 1). Excellent agreement between theory and experiment was obtained for the $\mathbf{A}(^{187}Re)$ matrix using the hybrid B3LYP functional. The inclusion of SOC terms had a significant impact on the magnitude of $A_{zz}(^{187}Re)$ (Table S2 in the Supporting Information). As predicted from earlier EPR studies,[8] the small hyperfine interaction is responsible for the appearance of the "shoulder" features in the randomly oriented CW-EPR spectra of these compounds (Figures 1b and 2b). Consistent with the approximate C_3 symmetry, both **A** and **Q** were nearly axial for both complexes, with their principal z axes directed within less than 0.5° of the molecular Z axis. The orientations of the principal g axes were less well-defined, a consequence of the small g anisotropy and nonideal symmetry of the crystal structure (Tables S1 and S2 in the Supporting Information).

The calculations further predicted a significant **Q** interaction for ^{187}Re relative to the comparatively small **A** (Table 1). The electric field gradient at the ^{187}Re nucleus was only a factor of ~2 greater than ^{99}Tc, with the larger $^{185,187}Re$ quadrupole coupling constant [$Q(^{187}Re) = 2.070$ barn vs $Q(^{99}Tc) = -0.129$ barn][17] and the smaller nuclear spin ($^{Re}I = {}^5/_2$ vs $^{Tc}I = {}^9/_2$) accounting for a factor of > 50 difference in **Q** for these two nuclei (eq 4 in the Supporting Information). Guided by theoretical predictions, empirical simulations of the EPR spectra of $Re(abt)_3$ using *XSophe*[21] program indicated that the comparatively large **Q** accounts for the unusual "satellite" lines due to formally forbidden $\Delta M_I > 0$ transitions that flank the narrower shoulder features (Table 1 and Figure 1). Nuclear quadrupole terms of similar magnitude have recently been obtained from empirical simulation of the neutral $Re(bdt)_3$ complex.[18] Electron-spin transient nutation experiments (not shown) provided no evidence to support an assignment of $S = 1$ (dimeric) or $S = {}^3/_2$ (trimeric) spin-coupled species previously proposed to account for the satellite lines.[8] A comparison of the simulated SH parameters for $Re(abt)_3$ in a frozen solution with

(14) (a) Huzinaga, S.; Miguel, B. *Chem. Phys. Lett.* **1990**, *175*, 289. (b) Huzinaga, S.; Klobukowski, M. *Chem. Phys. Lett.* **1993**, *212*, 260.
(15) (a) van Lenthe, E.; Baerends, E. J.; Snijders, J. G. *J. Chem. Phys.* **1993**, *99*, 4597–4610. (b) van Lenthe, E.; Baerends, E. J.; Snijders, J. G. *J. Chem. Phys.* **1996**, *105*, 6505–6516. (c) van Lenthe, E.; van der Avoird, A.; Wormer, P. E. S. *J. Chem. Phys.* **1998**, *108*, 4783–4796.
(16) Schrauzer, G. N.; Mayweg, V. P. *J. Am. Chem. Soc.* **1966**, *88*, 3235–3242.
(17) Pyykkö, P. *Mol. Phys.* **2001**, *99*, 1617–1629.
(18) Sproules, S.; Benedito, F. L.; Bill, E.; Weyhermüller, T.; DeBeer George, S.; Wieghardt, K. *Inorg. Chem.* **2009**, *48*, 10926–10941.

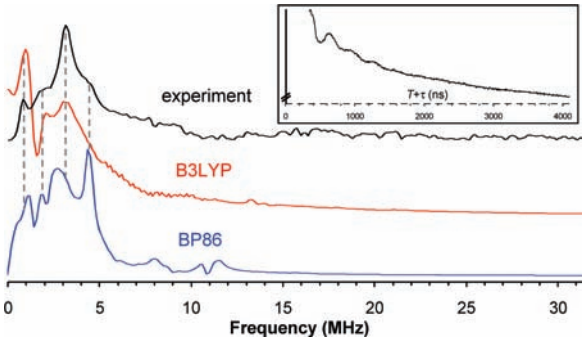

Figure 3. Comparison of experimental three-pulse ESEEM of $Re(abt)_3$ and simulations using the ^{14}N ligand hyperfine and quadrupole parameters computed from DFT (Tables S3−S6 in the Supporting Information). The strongly coupled ($a_{iso} > 2\nu_N$) ^{14}N ligand nuclei generate observable features between 0 and 10 MHz. Inset: experimental time domain signal. Experimental and simulated parameters: 9.71 GHz, 3 K, $\tau = 200$ ns, $B_0 = 3445$ G (absorption maximum), $t_{\pi/2} = 16$ ns, $\Delta t = 16$ ns, $T_1 = 5\ \mu$s.

the theoretical parameters shows good quantitative agreement with the hybrid B3LYP data, while the experimental g values are best predicted using the pure BP86 functional.

The presence of ^{14}N ligand nuclei also enabled the magnetic orbital of $Re(abt)_3$ to be probed using electron spin-echo envelope modulation (ESEEM) spectroscopy. Although the unpaired electron is strongly delocalized, the relaxation times were short ($T_1 \sim 5\ \mu$s at 3 K) and temperatures at or below 4 K were required to generate a detectable spin echo. The experimental stimulated ESEEM exhibited a broad spectrum with a maximum near 3.0 MHz (Figure 3). Depending on the choice of the functional, the theoretical $\mathbf{A}(^{14}N)$ and $\mathbf{Q}(^{14}N)$ parameters indicated a highly anisotropic hyperfine interaction ($T \sim 7-10$ MHz) and a_{iso} in the range 3−7 MHz (Tables S3−S6 in the Supporting Information). Simulations of the ESEEM spectrum using *Easyspin*[19] indicated that the B3LYP ligand parameters offer a satisfactory reproduction of the resolved experimental features, allowing for the difficulty in detecting low-frequency echo modulation because of the weak modulation depth (Figure 3, inset) and neglect of solvent polarity effects.

The EPR spectrum of a dilute frozen solution of $Tc(abt)_3$ in 9:1 dimethylformamide (DMF)/$CHCl_3$ showed prominent shoulder features but no evidence of satellite lines with an intensity greater than 0.2% of the shoulder features or of a central resonance (Figure 2). Empirical simulation of the X-band CW-EPR spectra of dilute (< 5 mM) frozen solutions indicated that the quadrupole interaction has no detectable influence on the spectrum provided that $Q_{zz} < 0.6 \times 10^{-4}$ cm^{-1}. This is in excellent agreement with the DFT calculations, in which $Q_{zz} < 0.5 \times 10^{-4}$ cm^{-1}, 2 orders of magnitude smaller than that for $Re(abt)_3$ (Table 1). The theoretical A_{xx} and A_{yy} values differ from the experiment by $< 1 \times 10^{-4}$ cm^{-1}; the deviation of the A_{zz} component is larger, although the experimental value lies between those calculated using BP86 and B3LYP functionals (Table 1).

More concentrated frozen solutions of $Tc(abt)_3$ show evidence for solute aggregation, as described by Baldas et al.[8] Most strikingly, the complex exhibits a central resonance that increases in intensity at greater solute concentrations;[8] however, no accompanying satellite lines have ever been observed. The excellent prediction of the experimental SH parameters of both $Tc(abt)_3$ and $Re(abt)_3$ using the in vacuo crystallographic structures, together with the experimental invariance of the shoulder and satellite resonances in a wide range of solvent compositions,[8] indicates that the metal **A** and **Q** interactions are unlikely to be modulated by the solvent polarity. Because the quadrupole interaction is presently shown both theoretically and experimentally to be $< 0.6 \times 10^{-4}$ cm^{-1}, a concentration-dependent central resonance in $Tc(abt)_3$ spectra can only be explained by weak intermolecular exchange interactions that become enhanced at higher solute concentrations. The width of the central resonance in $Re(abt)_3$ is also broadened at solute concentrations > 5 mM, suggesting that aggregation and weak intermolecular exchange also occurs in this complex.[8] Some dithiolene complexes of molydenum and tungsten, with delocalized spin density and close face-to-face contacts between monomeric units in the solid state, exhibit antiferromagnetic interactions.[20] Because close face-to-face contacts (< 3.5 Å) are also present in the crystallographic structures of trigonal-prismatic technetium and rhenium complexes,[9,12] it is possible that similar behavior occurs for $Tc(abt)_3$ and $Re(abt)_3$ because of the formation of locally high solute concentrations upon freezing. The present study has demonstrated quantitative predictions of the magnetic resonance parameters of the dilute complexes using relativistic DFT. Further investigation of intermolecular interactions will require modeling of an extended molecular structure.

Supporting Information Available: Listings of experimental methods, computational details, theoretical ligand ^{14}N hyperfine and quadrupole parameters, Euler angles, SOC contributions to metal hyperfine parameters, and spin-density plots. This material is available free of charge via the Internet at http://pubs.acs.org.

(19) (a) Stoll, S.; Schweiger, A. *J. Magn. Reson.* **2006**, *178*, 42–55. (b) Stoll, S.; Britt, R. D. *Phys. Chem. Chem. Phys.* **2009**, *11*, 6614–6625.

(20) Domercq, B.; Coulon, C.; Fourmigué, M. *Inorg. Chem.* **2001**, *40*, 371–378.

(21) Hanson, G. R.; Gates, K. E.; Noble, C. J.; Griffin, M.; Mitchell, A.; Benson, S. *J. Inorg. Biochem.* **2004**, *98*, 903–916.